

Resistive detection of nuclear spins in a single quantum dot under Kondo effect regime

M. Kawamura,^{1,2} D. Gottwald,¹ K. Ono,¹ T. Machida,^{3,4} and K. Kono¹

¹*RIKEN Advanced Science Institute, Saitama 351-0198, Japan**

²*PRESTO, Japan Science and Technology Agency, Saitama 333-0012, Japan*

³*Institute of Industrial Science, University of Tokyo, Tokyo 153-8505, Japan*

⁴*Institute for Nano Quantum Information Electronics, University of Tokyo, Tokyo 153-8505, Japan*

(Dated: April 26, 2022)

We study dynamic polarization and resistive detection of nuclear spins in a semiconductor quantum dot (QD) under the Kondo effect regime. We find that the differential conductance spectra of the QD exhibit hysteresis under the Kondo effect regime in magnetic fields. Relevance of nuclear spins to the hysteresis is confirmed by the detection of nuclear magnetic resonance signals by monitoring the differential conductance. We attribute the origin of the hysteresis to the dynamic nuclear spin polarization (DNP) induced in the QD. Using the DNP, we demonstrate nuclear spin relaxation rate measurements in the QD under the Kondo effect regime.

PACS numbers: 73.63.Kv, 72.10.Fk, 76.60.-k

The Kondo effect, arising from the interaction between a localized spin and itinerant spins at the Fermi energy, is one of the most fundamental many-body phenomena observed in semiconductor quantum dot (QD) systems¹⁻⁴. The differential conductance (dI/dV_{sd}) spectrum of the QD exhibits a sharp zero-bias conductance peak (ZBCP), which reflects the Kondo resonance at the Fermi energy. In the presence of an external magnetic field B , the energy for the Kondo resonance shifts away from the Fermi energy by $\pm|g^*|\mu_B B$ due to the Zeeman splitting of the electronic state in the QD¹, where g^* is the effective g-factor for electrons and μ_B is the Bohr magneton. Consequently, the dI/dV_{sd} spectrum splits into two peaks at finite bias voltages. The peak-to-peak voltage V_{p-p} , defined as the difference in the bias voltage between the split differential conductance peaks, is given by twice the Zeeman energy^{1,3} $V_{p-p} = 2|g^*|\mu_B B/e$.

Because an electron spin \vec{S} in a semiconductor device can interact with a nuclear spin \vec{I} of the host material through the contact hyperfine interaction $H_{hyp} = A\vec{I} \cdot \vec{S} = A(I^+S^- + I^-S^+)/2 + A I_z S_z$, where A is the hyperfine coupling constant, a dynamic nuclear spin polarization (DNP) can be build by driving electron spins using optical or electrical means^{5,6}. The polarized nuclear spins modify the Zeeman energy for electrons through an effective magnetic field $B_N = A\langle I_z \rangle / g^* \mu_B$ [Fig. 1(a)]. In a QD under the Kondo effect regime, the modification of the Zeeman energy is expected to change the peak-to-peak voltage V_{p-p} between the split dI/dV_{sd} peaks to $V_{p-p} = 2|g^*|\mu_B(B + B_N)/e$, as shown schematically in Fig. 1(b). Therefore a small change in the nuclear spin polarization can be sensitively detected by measuring the dI/dV_{sd} spectrum. However, to the best of our knowledge, effects of nuclear spins on transport properties of a QD under the Kondo effect regime have not been addressed experimentally. In addition, establishment of a novel technique for the resistive detection of nuclear spins has a potential to open a way for studying electron spin

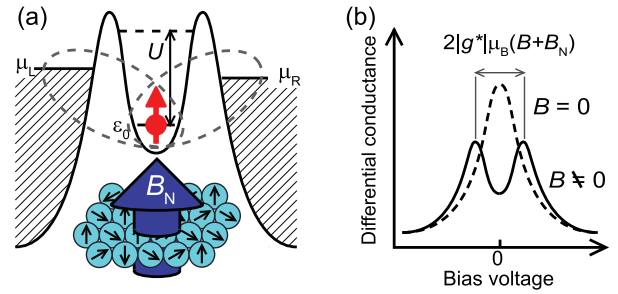


FIG. 1: (color online). (a) Schematic of a QD with nuclear spins. An electron spin in the QD is influenced by an effective magnetic field B_N produced by the nuclear spins. (b) Schematic of differential conductance spectra in a QD under the Kondo effect regime. Application of an external magnetic field B causes the splitting of the dI/dV_{sd} spectrum. The peak-to-peak voltage between the split dI/dV_{sd} peaks is further modified by B_N .

properties in a QD through nuclear magnetic resonance (NMR) measurements.

In this paper, we report dynamic polarization and resistive detection of nuclear spins in a single QD under the Kondo effect regime. We find that the dI/dV_{sd} spectra exhibit hysteresis under the Kondo effect regime in magnetic fields. We also find that the value of dI/dV_{sd} evolves slowly at the bias voltages between the split dI/dV_{sd} peaks. Relevance of nuclear spins to the hysteresis and the slow evolution of dI/dV_{sd} is confirmed by the detection of NMR signals by monitoring dI/dV_{sd} . We attribute the origin of the hysteresis and the slow evolution of dI/dV_{sd} to the DNP induced in the QD. Using the DNP, we demonstrate nuclear spin relaxation rate measurements in the QD under the Kondo effect regime.

We prepared QDs using a wafer of GaAs/Al_{0.3}Ga_{0.7}As single heterostructure with a two-dimensional electron gas (2DEG) at the interface. The carrier density and

mobility of the 2DEG are $n = 2.3 \times 10^{15} \text{ m}^{-2}$ and $\mu = 17 \text{ m}^2/\text{Vs}$, respectively. The QDs were made using split-gate devices [inset of Fig. 2(e)], following the approach in Refs. 7 and 8; QDs form occasionally in split-gate devices near the pinch-off conditions in the presence of disorder⁹, and some of them exhibit the Kondo effect^{7,8}. The devices were cooled using a dilution refrigerator and magnetic fields were applied parallel to the plane of the 2DEG. A standard lock-in technique with an excitation voltage of $10 \text{ } \mu\text{V}$ and a frequency of 18 Hz was used to measure dI/dV_{sd} applying a bias voltage V_{sd} between the source and drain electrodes.

Figure 2(a) shows the gate voltage V_g dependence of the conductance of one of the devices. The conductance decreases with decreasing V_g , and several conductance peaks appear before the pinch-off, indicating formation of a QD at the constriction. The transport properties of the device exhibit behavior typical of the Kondo effect in a QD^{2,3}. (1) The conductance shows an increase with decreasing temperature T at a conductance minimum in the $dI/dV_{\text{sd}}-V_g$ curve and the opposite temperature dependence at the neighboring conductance minimum [Fig. 2(a)]. (2) A pronounced ZBCP in the $dI/dV_{\text{sd}}-V_{\text{sd}}$ curve develops with decreasing temperature below 700 mK [Fig. 2(b)]. The ZBCPs appear as a bright colored ridge in the gray-scale plot of dI/dV_{sd} as a function of V_g and V_{sd} [Fig. 2(c)]. (3) The dI/dV_{sd} spectrum splits into two peaks under in-plane magnetic fields B [Fig. 2(e)], accompanied by the splitting of the dI/dV_{sd} ridge [Fig. 2(d)]. The peak-to-peak voltage $V_{\text{p-p}}$ between the split dI/dV_{sd} peaks is almost independent of V_g as expected from the theory of the Kondo effect in a QD¹. The value of $V_{\text{p-p}}$ increases with increasing B , showing an agreement with theoretically expected values of $V_{\text{p-p}} = 2|g^*|\mu_B B/e$ with $|g^*| = 0.44$ for GaAs, as marked by triangles in Fig. 2(e).

We find that remarkable hysteresis appears in the dI/dV_{sd} spectra under magnetic fields; the $dI/dV_{\text{sd}}-V_{\text{sd}}$ curve of the positive scan ($dV_{\text{sd}}/dt > 0$) appears above that of the negative scan ($dV_{\text{sd}}/dt < 0$) as shown in Fig. 2(e). The $dI/dV_{\text{sd}}-V_{\text{sd}}$ curves shown in Fig. 2(e) are obtained by scanning V_{sd} between $-500 \text{ } \mu\text{V}$ and $+500 \text{ } \mu\text{V}$ in positive and negative directions at a rate of $5 \text{ } \mu\text{V/s}$. The hysteresis appears in a particular range of V_{sd} between the dI/dV_{sd} peaks at each magnetic field. The hysteresis in the $dI/dV_{\text{sd}}-V_{\text{sd}}$ curves indicates involvement of a phenomenon with a long relaxation time in the mechanism of electron transport.

Figure 3(a) shows representative data describing the temporal change in dI/dV_{sd} at $B = 2.88 \text{ T}$ after a rapid change of V_g and V_{sd} from the pinch-off condition to $(V_g, V_{\text{sd}}) = (-0.65 \text{ V}, -40 \text{ } \mu\text{V})$ on the slope of the dI/dV_{sd} peak. The value of dI/dV_{sd} increases continuously over a period of 150 s . The long time required to change dI/dV_{sd} in Fig. 3(a) is in accordance with the typical time scale for building up a DNP in GaAs¹⁰⁻¹⁷, suggesting the occurrence of the DNP in the present QD.

Relevance of the nuclear spins to the hysteresis and

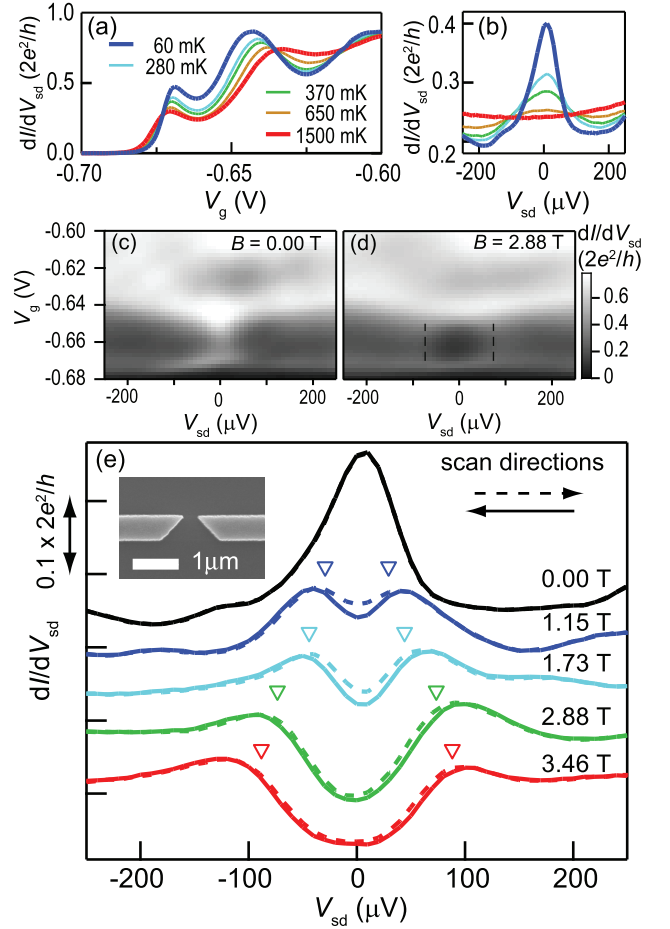


FIG. 2: (color online). (a) Dependence of dI/dV_{sd} on V_g at $V_{\text{sd}} = 0 \text{ } \mu\text{V}$ under temperatures $T = 60, 280, 370, 650,$ and 1500 mK . (b) Dependence of dI/dV_{sd} on V_{sd} at $V_g = -0.66 \text{ V}$ under various temperatures. The temperatures are the same as in (a). (c) and (d) Gray-scale plot of dI/dV_{sd} as a function of V_g and V_{sd} for $B = 0.00 \text{ T}$ (c) and 2.88 T (d). Dashed lines in (d) indicate the theoretically expected position of dI/dV_{sd} peaks $\pm|g^*|\mu_B B/e$. (e) Dependence of dI/dV_{sd} on V_{sd} at $V_g = -0.66 \text{ V}$ and $T = 30 \text{ mK}$ under magnetic fields $B = 0.00, 1.15, 1.73, 2.88,$ and 3.46 T . The curves are offset by $0.06 \times 2e^2/h$. The expected voltage positions of dI/dV_{sd} peaks are marked by triangles. The solid and dashed curves represent the data for the positive and negative scans, respectively. Inset shows scanning electron micrograph of the split-gate device.

the slow evolution of dI/dV_{sd} is confirmed by the following NMR spectroscopy measurement. We apply continuous waves of radio-frequency (rf) magnetic fields using a single-turn coil wound around the device. The frequency f of the rf-magnetic field is scanned after the saturation of dI/dV_{sd} at $(V_g, V_{\text{sd}}) = (-0.65 \text{ V}, -40 \text{ } \mu\text{V})$. As shown in Fig. 3(b), the value of dI/dV_{sd} decreases when the frequency matches the NMR frequencies of ^{75}As (gyromagnetic ratio $\gamma = 45.82 \text{ rad-MHz/T}$). The NMR spectrum of ^{75}As is obtained¹⁸ by monitoring dI/dV_{sd} . The NMR spectra of ^{69}Ga and ^{71}Ga are also obtained (not

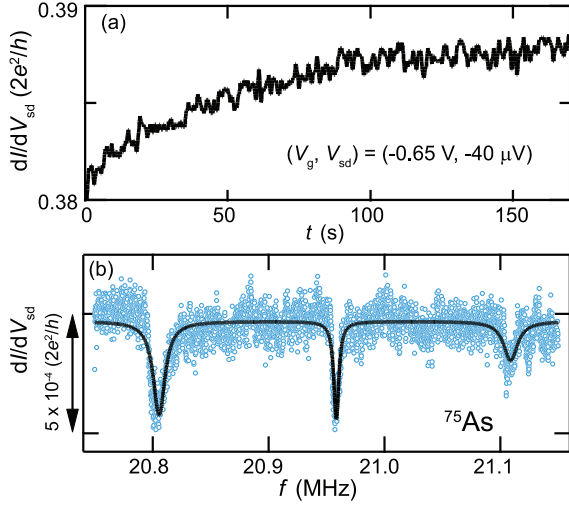


FIG. 3: (color online). (a) Temporal change of dI/dV_{sd} at $(V_g, V_{sd}) = (-0.65 \text{ V}, -40 \mu\text{V})$ and $B = 2.88 \text{ T}$ after a rapid change in V_g and V_{sd} from the pinch-off condition $(V_g, V_{sd}) = (-0.70 \text{ V}, 0 \mu\text{V})$. (b) NMR spectrum of ^{75}As obtained by monitoring dI/dV_{sd} at $(V_g, V_{sd}) = (-0.65 \text{ V}, -40 \mu\text{V})$ and $B = 2.88 \text{ T}$ under irradiation of rf-magnetic field. Black curve is the Lorentzian fitting result. The splitting of the spectrum is due to the electric quadrupole interaction of the nuclei.

shown). The observed decreases in dI/dV_{sd} correspond to the decreases in the nuclear spin polarization due to the absorption of rf-magnetic fields at the NMR frequencies. Thus, the changes in the nuclear spin polarization are detected by measuring dI/dV_{sd} under the Kondo effect regime as expected [Fig. 1(b)].

Because dI/dV_{sd} reflects changes in the nuclear spin polarization, the slow increase of dI/dV_{sd} in Fig. 3(a) is interpreted as the development of the DNP in the present QD. The possibilities of the electron heating or the drift of the gate voltages are ruled out from the origin of the hysteresis and the slow evolution of dI/dV_{sd} because of the absence of the hysteresis at $B = 0.00 \text{ T}$. The induced DNP modifies the dI/dV_{sd} spectra through the Zeeman energy, changing the peak-to-peak voltage to $V_{p-p} = 2|g^*|\mu_B(B + B_N)/e$. Because the DNP develops during the scans of V_{sd} in the dI/dV_{sd} - V_{sd} measurements in Fig. 2(e), the resultant difference in the nuclear spin polarization at the same V_{sd} causes the hysteresis in the dI/dV_{sd} - V_{sd} curves. We think that coexistence of the DNP and the Kondo effect is allowed because the electron-nuclear flip-flop process of the DNP does not interfere with the formation of the Kondo singlet significantly due to the small characteristic energy for the flip-flop process ($\sim 1 \text{ neV}$)^{19,20} compared to that for the Kondo effect ($k_B T_K \sim 80 \mu\text{eV}$).

The above described mechanism of the hysteresis is based on the sensitivity of the dI/dV_{sd} spectra to the changes in the Zeeman energy. Therefore the conditions for the hysteresis to occur is expected to be related to the appearance of the Kondo effect. Figure 4(a) shows

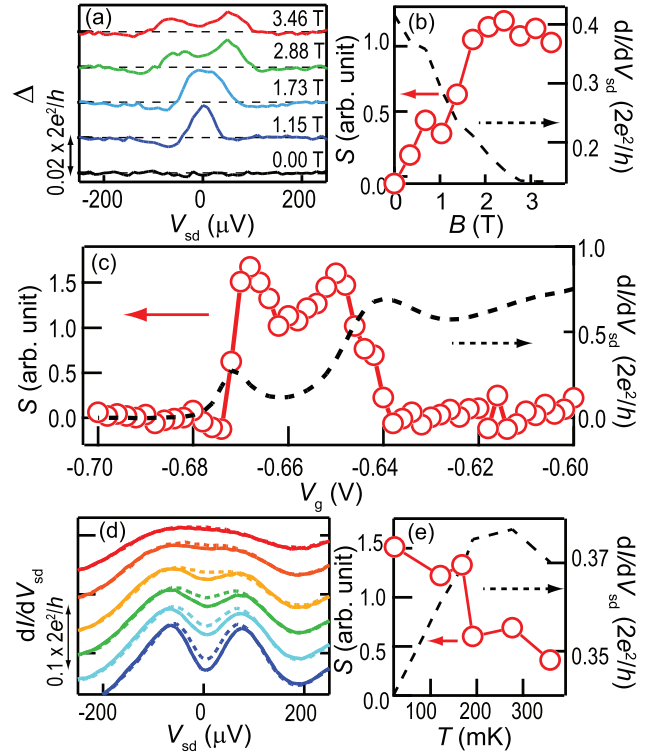


FIG. 4: (color online). (a) Hysteresis Δ defined as the difference in dI/dV_{sd} between the positive and negative scans of V_{sd} in Fig. 2(e). The Δ - V_{sd} curves for $V_g = -0.66 \text{ V}$ at $B = 0.00, 1.15, 1.73, 2.88, \text{ and } 3.46 \text{ T}$ are shown. The curves are offset by $0.02 \times 2e^2/h$. (b) Magnetic field dependences of the area S of the hysteresis (open circles, left axis) and $dI/dV_{sd}(V_{sd} = 0 \mu\text{V})$ (dashed curve, right axis) at $V_g = -0.66 \text{ V}$ and $T = 30 \text{ mK}$. (c) Gate voltage dependences of S (open circles, left axis) and $dI/dV_{sd}(V_{sd} = 0 \mu\text{V})$ (dashed curve, right axis) at $B = 2.88 \text{ T}$ and $T = 30 \text{ mK}$. (d) The dI/dV_{sd} - V_{sd} curves for $V_g = -0.65 \text{ V}$ and $B = 2.88 \text{ T}$ under various temperatures $T = 60, 120, 170, 190, 280, \text{ and } 360 \text{ mK}$ from bottom to top. The solid and dashed curves represent the data for the positive and negative scans, respectively. The curves are offset by $0.04 \times 2e^2/h$. (e) Temperature dependences of S (open circles, left axis) and $dI/dV_{sd}(V_{sd} = 0 \mu\text{V})$ (dashed curve, right axis) at $V_g = -0.65 \text{ V}$ and $B = 2.88 \text{ T}$.

the hysteresis Δ , defined as the difference in dI/dV_{sd} between the positive and negative scans of V_{sd} shown in Fig. 2(e). To discuss the conditions for the hysteresis to occur, we introduce the area S of the hysteresis by integrating the hysteresis Δ over a range $-200 \mu\text{V} \leq V_{sd} \leq 200 \mu\text{V}$. The area S , which is zero at $B = 0.00 \text{ T}$, increases with increasing B and becomes saturated above $B = 2 \text{ T}$ [Fig. 4(b)]. The dependence of S on V_g [Fig. 4(c)] reveals that the hysteresis is remarkable in a range of V_g where the Kondo effect appears ($-0.67 \text{ V} < V_g < -0.64 \text{ V}$). The values of S are almost zero at the other gate voltages. With increasing temperature T under a fixed magnetic field, the hysteresis becomes small and the value of S decreases as shown in Figs. 4(d) and 4(e).

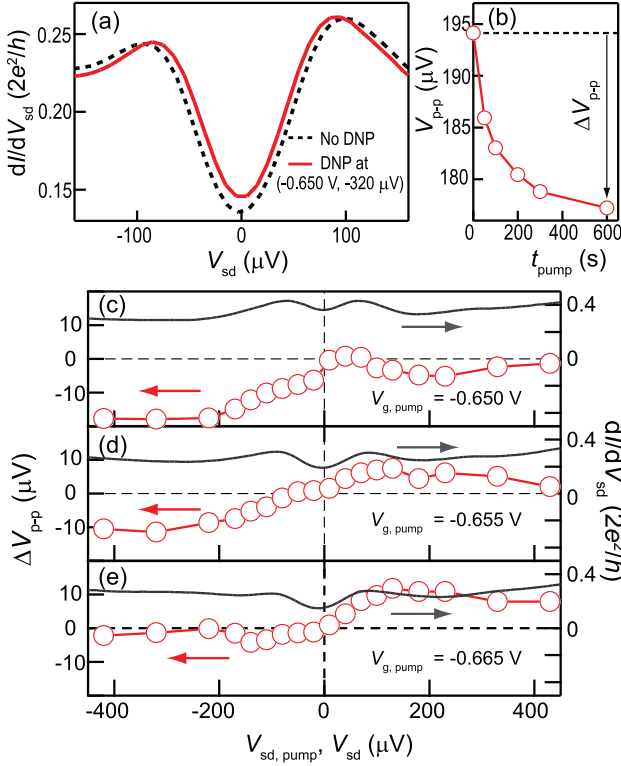


FIG. 5: (color online). (a) dI/dV_{sd} - V_{sd} curves at $V_g = -0.650$ V obtained without the DNP pumping (dashed) and after the DNP pumping (solid) for $t_{pump} = 600$ s. The DNP pumping voltages $(V_{g,pump}, V_{sd,pump}) = (-0.650$ V, $-320 \mu V)$. (b) Dependence of V_{p-p} on the DNP pumping period t_{pump} . The DNP pumping voltages are the same as in (a). The DNP is relaxed between each measurement by waiting more than 20 minutes under the pinch-off condition. (c)-(e) Dependence of ΔV_{p-p} on the DNP pumping voltages $(V_{g,pump}, V_{sd,pump})$ for $t_{pump} = 600$ s. The V_{sd} dependences of dI/dV_{sd} (solid curve) are plotted on the right axis.

The hysteresis almost disappears at around $T = 360$ mK, which is considerably lower than the onset temperature of the Kondo effect (about 700 mK). The temperature where the hysteresis disappears is close to the temperature where the splitting of the dI/dV_{sd} spectrum becomes unclear [Fig. 4(d)]. These observations show that the hysteresis is one of the unique features of the Kondo effect in the magnetic fields and that the differential conductance under the Kondo effect regime is sensitive to the changes in the effective magnetic field $B + B_N$.

The effect of the DNP on the dI/dV_{sd} spectra can be seen more directly in the following pump-probe measurement. The dashed and solid curves in Fig. 5(a) show the dI/dV_{sd} - V_{sd} curves at the same V_g . The dashed curve is obtained immediately after relaxing the nuclear spin polarization under the pinch-off condition and the solid curve is obtained after the DNP pumping at $(V_{g,pump}, V_{sd,pump}) = (-0.650$ V, $-320 \mu V)$ for $t_{pump} = 600$ s. The peak-to-peak voltage V_{p-p} after the DNP pumping

is smaller than that without the DNP pumping. With increasing the period of the DNP pumping t_{pump} , V_{p-p} decreases gradually, as shown in Fig. 5(b). The gradual change in V_{p-p} with increasing t_{pump} gives an additional evidence for the occurrence of the DNP. The shift ΔV_{p-p} measured from the value of V_{p-p} without the DNP pumping allows us to evaluate the effective magnetic field B_N using a proportional relation $\Delta V_{p-p}/V_{p-p} = B_N/(B + B_N)$, which is yielded based on an assumption $V_{p-p} = 2|g^*|\mu_B(B + B_N)/e$. A representative value of $\Delta V_{p-p} = -17.9 \mu V$ obtained from the difference between the dashed and solid curves in Fig. 5(a) corresponds to $B_N = -0.26$ T. This value is equivalent to the nuclear spin polarization of 4.9 % using the expression for B_N in GaAs obtained in Ref. 21.

Figures 5(c)-5(e) show the dependence of ΔV_{p-p} on the DNP pumping voltages $(V_{g,pump}, V_{sd,pump})$. The values of ΔV_{p-p} , which are proportional to B_N , are almost zero at around $V_{sd,pump} = 0$, while large values of $|\Delta V_{p-p}|$ are obtained at $|V_{sd}| > 100 \mu V$. In addition, the sign of ΔV_{p-p} , which indicates the DNP polarity, strongly depends on the DNP pumping voltage. The negative ΔV_{p-p} ($B_N < 0$) is remarkable at $V_{g,pump} = -0.650$ V with $V_{sd,pump} < 0$ [Fig. 5(c)], while the positive ΔV_{p-p} ($B_N > 0$) is remarkable at $V_{g,pump} = -0.665$ V with $V_{sd,pump} > 0$ [Fig. 5(e)]. At the gate voltage between them ($V_{g,pump} = -0.655$ V), both polarities appear depending on the sign of $V_{sd,pump}$ [Fig. 5(d)].

The optimum values of $|V_{sd,pump}|$ for the DNP pumping are larger than the $|V_{sd}|$ values for the dI/dV_{sd} peaks. Moreover, the $V_{sd,pump}$ range where the DNP is achieved does not coincide with the V_{sd} range where the hysteresis is observed. Both facts suggest that the mechanism for the DNP pumping is not directly related to that of the Kondo effect. In addition, the dependence of the DNP polarity on the sign of $V_{sd,pump}$ indicates that the present QD is asymmetric and that the asymmetry plays an important role in the DNP pumping mechanism. We think that the positive B_N could be attributed to the electron spin relaxation in the QD. When adding an electron to the empty QD, both up-spin and down-spin state are allowed. If the added electron is in the down-spin state, it can relax to the up-spin state in the QD before going to the electrode. The down-to-up flips of electron spins cause to decrease the nuclear spin polarization $\langle I_z \rangle$ via the electron-nuclear flip-flop process of the hyperfine interaction, building up the positive B_N in Fig. 5(e)²². Because of the asymmetric couplings between the QD and the electrodes, the added electron probably goes through the QD before relaxing its spin when $V_{sd,pump} < 0$. The negative B_N in Fig. 5(c) indicates involvement of the up-to-down flips of electron spins in the QD. At the present stage, we do not have a comprehensive explanation why the up-to-down flips become dominant as the gate voltage is increased. Further studies will be needed to fully understand the DNP pumping mechanism.

Impact of the newly developed techniques of the DNP and the resistive detection of nuclear spins is further em-

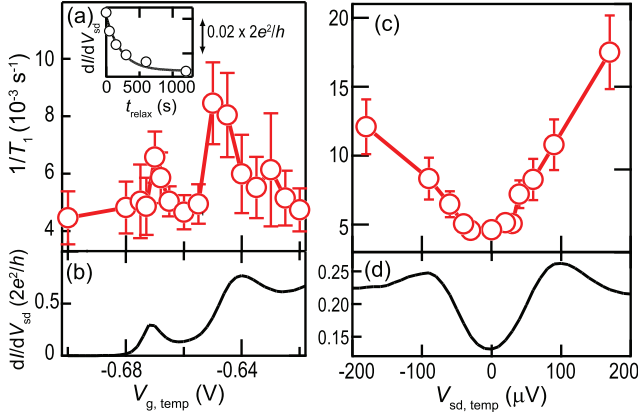


FIG. 6: (color online). (a) Dependence of $1/T_1$ on $V_{g,temp}$ for $V_{sd,temp} = 0 \mu\text{V}$ and $B = 2.88 \text{ T}$. Inset shows a representative decay curve of the nuclear spin polarization at the pinch-off condition $(V_{g,temp}, V_{sd,temp}) = (-0.70 \text{ V}, 0 \mu\text{V})$. (b) dI/dV_{sd} - V_g curve at $V_{sd} = 0 \mu\text{V}$. (c) Dependence of $1/T_1$ on $V_{sd,temp}$ for $V_{g,temp} = -0.66 \text{ V}$ and $B = 2.88 \text{ T}$. (d) dI/dV_{sd} - V_{sd} curve at $V_g = -0.66 \text{ V}$.

phasized by the following nuclear spin relaxation rate $1/T_1$ measurements. Because $1/T_1$ is enhanced by the electron spin fluctuation, the electron spin dynamics in the QD can be studied through the $1/T_1$ measurements. The decay curve of nuclear spin polarization is obtained by the following procedure: First, the DNP is pumped at $(V_g, V_{sd}) = (-0.650 \text{ V}, -320 \mu\text{V})$. Then, the nuclear spin polarization is relaxed under a certain voltage condition $(V_{g,temp}, V_{sd,temp})$ for a given time t_{relax} . Finally, the change in the nuclear spin polarization is

read out by monitoring dI/dV_{sd} at $(-0.650 \text{ V}, 0 \mu\text{V})$. By repeating this procedure with different periods t_{relax} , we obtain the decay curve of the nuclear spin polarization as shown in the inset of Fig. 6(a). The value of $1/T_1$ is evaluated by fitting the decay curve to the form $dI/dV_{sd} = a + b \exp(-t_{relax}/T_1)$.

Figure 6(a) shows the dependence of $1/T_1$ on $V_{g,temp}$ at $B = 2.88 \text{ T}$ for $V_{sd,temp} = 0 \mu\text{V}$. The relaxation rate $1/T_1 = 4.4 \times 10^{-3} \text{ s}^{-1}$ for $V_{g,temp} = -0.70 \text{ V}$ (the QD is depleted during the relaxation) is in the same order as the reported $1/T_1$ values in GaAs¹³. The relaxation rate increases as $V_{g,temp}$ approaches the conductance peaks [Fig. 6(b)]. We think that electron spin fluctuations introduced by the electron tunneling cause the increase in $1/T_1$. The small values of $1/T_1$ at around $V_{g,temp} = -0.66 \text{ V}$ can be attributed to the suppression of the electron spin fluctuation due to the Zeeman effect. When a bias voltage $V_{sd,temp}$ is applied during the relaxation [Fig. 6(c)], the values of $1/T_1$ do not increase largely at $|V_{sd,temp}| < 40 \mu\text{V}$. $1/T_1$ becomes large at $|V_{sd,temp}| > 40 \mu\text{V}$ associated with the increase in dI/dV_{sd} [Fig. 6(d)]. The increase in $1/T_1$ is probably related to the electron transport through the Kondo resonance state. We think that the $1/T_1$ measurement using the DNP technique is useful to understand spin properties of the Kondo effect under the non-equilibrium regime.

This work was supported by the PRESTO of JST, Grant-in-Aid for Scientific Research from the MEXT, and the Project for Developing Innovation Systems of the MEXT. We thank M. Eto, T. Kubo, S. Amaha, and E. Minamitani for helpful discussions. D. G. acknowledges the RIKEN-Konstantz Univ. internship program.

* Electronic address: minoru@riken.jp

- ¹ Y. Meir, N. S. Wingreen, and P. A. Lee, Phys. Rev. Lett. **70**, 2601 (1993).
- ² D. Goldhaber-Gordon *et al.*, Nature (London) **391**, 156 (1998).
- ³ S. M. Cronenwett, T. H. Oosterkamp, and L. P. Kouwenhoven, Science **281**, 540 (1998).
- ⁴ W. G. van der Wiel *et al.*, Science **289**, 2105 (2000).
- ⁵ A. Abragam, *Principles of Nuclear Magnetism* (Oxford University Press, 1984).
- ⁶ C. P. Slichter, *Principles of Magnetic resonance 3rd eds.* (Springer, 1990).
- ⁷ F. Sfigakis *et al.*, Phys. Rev. Lett. **100**, 026807 (2008).
- ⁸ O. Klochan *et al.*, Phys. Rev. Lett. **107**, 076805 (2011).
- ⁹ P. L. McEuen, B. W. Alphenaar, R. G. Wheeler, and R. N. Sacks, Surf. Sci. **229**, 312 (1990).
- ¹⁰ K. R. Wald, L. P. Kouwenhoven, P. L. McEuen, N. C. van der Vaart, and C. T. Foxon, Phys. Rev. Lett. **73**, 1011 (1994).
- ¹¹ T. Machida *et al.*, Appl. Phys. Lett. **80**, 4178 (2002).

- ¹² S. Kronmüller *et al.*, Phys. Rev. Lett. **81**, 2526 (1998).
- ¹³ K. Hashimoto, K. Muraki, T. Saku, and Y. Hirayama, Phys. Rev. Lett. **88**, 176601 (2002).
- ¹⁴ Y. Ren, W. Yu, S. M. Frolov, J. A. Folk, and W. Wegscheider, Phys. Rev. B **81**, 125330 (2010).
- ¹⁵ M. Kawamura *et al.*, Appl. Phys. Lett. **90**, 022102 (2007).
- ¹⁶ M. Kawamura *et al.*, Phys. Rev. B **79**, 193304 (2009).
- ¹⁷ K. Ono & S. Tarucha, Phys. Rev. Lett. **92**, 256803 (2004).
- ¹⁸ NMR spectra are not obtained at bias and gate voltage conditions where the hysteresis is not observed.
- ¹⁹ W. A. Coish and J. Baugh, Phys. Status Solidi B **246**, 2203 (2009).
- ²⁰ We assume the averaged hyperfine coupling constant $A = 90 \mu\text{eV}$ for GaAs²¹ and 10^5 nuclei in the QD.
- ²¹ D. Paget, G. Lampel, B. Sapoval, and V. I. Safarov, Phys. Rev. B **15**, 5780 (1977).
- ²² Because $g^* < 0$ and $A > 0$ in GaAs, a negative nuclear spin polarization $\langle I_z \rangle < 0$ corresponds to $B_N > 0$.